Microfluidic Simulations of Micropump with Multiple Vibrating Membranes

K. Koombua[*], R. M. Pidaparti[**], P. W. Longest[***], and G. M. Atkinson[****]

[*]Department of Mechanical Engineering, Virginia Commonwealth University, Richmond, VA 23284, USA, koombuak@vcu.edu
[**]Department of Mechanical Engineering, Virginia Commonwealth University, Richmond, VA 23284, USA, rmpidaparti@vcu.edu
[***]Department of Mechanical Engineering, Virginia Commonwealth University, Richmond, VA 23284, USA, pwlongest@vcu.edu
[****]Department of Electrical and Computer Engineering, Virginia Commonwealth University, Richmond, VA 23284, USA, gmatkins@vcu.edu

ABSTRACT

A novel design of a micropump with multiple vibrating membranes has been investigated in this study. The micropump consists of three nozzle/diffuser elements with vibrating membranes, which are used to create pressure difference in the pump chamber. The dynamic mesh algorithm in the computational fluid dynamics solver, FLUENT, was employed to study transient responses of fluid velocity and flow rate during the operating cycle of the micropump. The design simulation results showed that the movement of wall membranes combined with the rectification behavior of three nozzle/diffuser elements can minimize back flow and improve net flow in one direction. The maximum flow rate from the micropump increased when the membrane displacement and membrane frequency increased. Based on the performance characteristics from the simulations, the designed micropump is suitable to fabricate for practical applications.

Keywords: Valveless micropump; Nozzle/diffuser elements; vibrating membrane; Computational fluid dynamics

1 INTRODUCTION

A micropump is a primary component of many microfluidic systems and can be used to control the movement of small fluid volumes. Applications of the micropumps include implantable drug delivery systems [1], insulin injectors [2], artificial prostheses [3], liquid cooling systems [4], fuel cells [5], as well as macromolecule and cell analysis [6].

The main disadvantage of the current valveless micropump is overpressure at the outlet can cause a back flow to occur throughout the operating cycle [7]. This reverse flow decreases the average flow rate from the micropump and leads to an increase in energy consumption. In this study, a micropump consisting of three nozzle/diffuser elements with multiple membranes was designed to improve net flow in one direction. The fluidic characteristics of the micropump were analyzed implementing the CFD simulations.

2 MICROPUMP DESIGN

In contrast to the existing valveless micropumps, we propose a new technique to improve unidirectional fluid flow using three nozzle/diffuser elements with multiple vibrating membranes. The proposed design of the micropump is shown in Figure 1. The micropump consists of four components: microfluidic chip, pump chamber, actuator unit, and top cover. The pump chamber of the micropump has an hourglass shape and consists of membranes 1, 2, and 3 and chambers 1, 2, and 3. The dimensions of the pump chamber are approximately 2 mm x 1 mm x 50 μm (see Figure 2). The actuator unit can be made of a piezoelectric material. The movement of this piezoelectric material can be accurately controlled by an applied voltage. Change in length and curvature of the piezoelectric material results in the movement of membranes 1, 2, and 3 of the pump chamber and lead to decrease or increase in a volume of the pump chamber. Movement of these membranes can potentially minimize back flow and improve net flow in one direction.

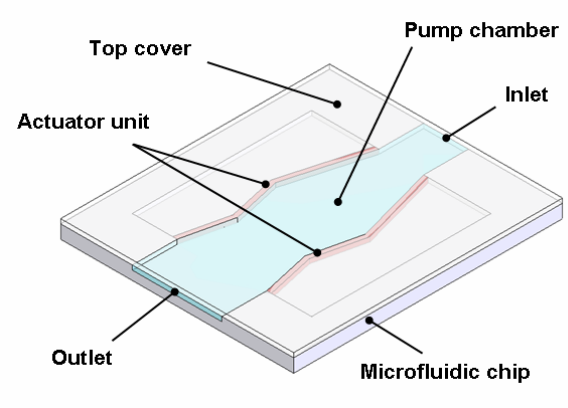

Figure 1: A design of the micropump with multiple vibrating membranes.

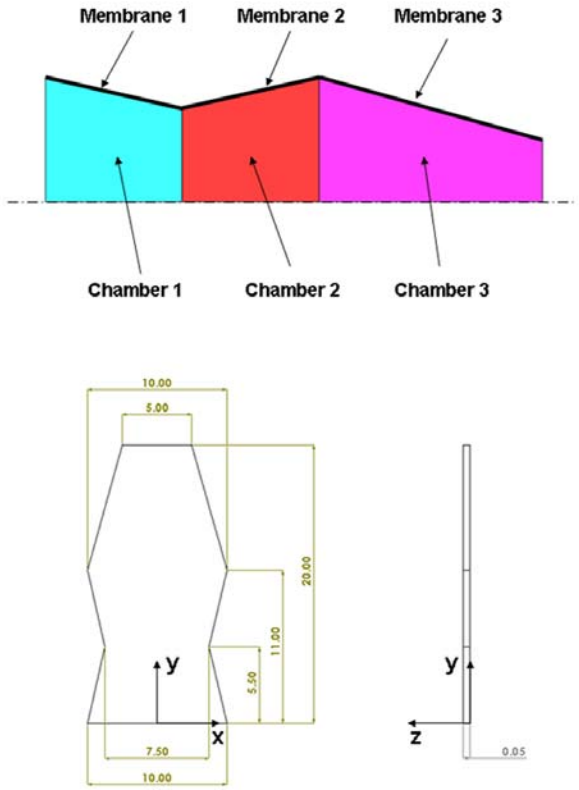

Figure 2: A schematic diagram of the pump chamber (top). Due to symmetry, only a half portion of the pump chamber is shown. Detail geometry of the pump chamber (bottom). All units are in mm.

The unique performance characteristics of the proposed micropump result from a specific sequence of membrane motion. For pumping mode, Fluid moves from chambers 2 and 3 to chamber 1 and to the outlet when membranes 2 and 3 move down and membrane 1 move up. These movements generate low pressure in chamber 1 and high pressure in chambers 2 and 3 (see Figure 3). In supply mode, fluid is drawn from the inlet into chambers 2 and 3 due to low pressure when membranes 2 and 3 move up. At the same time, membrane 1 moves down and generate high pressure in chamber 1. This high pressure minimizes a reverse flow from the outlet into the chamber 1 (see Figure 3).

3 MICROPUMP MODELING

The commercial computational fluid dynamics software FLUENT, was used to simulate a transient response of fluid flow within the micropump. This software uses a finite volume method to discretise the Navier-Stokes equations that describe the exchange of mass, momentum, and energy through the boundary of a control volume, which is fixed in space. The Navier-Stokes equations in the integral formulation that describes the fluid dynamics were shown below [8].

$$\frac{\partial}{\partial t}\int_{\Omega}\vec{W}d\Omega+\oint_{\partial\Omega}\left(\vec{F}_c-\vec{F}_v\right)dS=\int_{\Omega}\vec{Q}\,d\Omega \qquad (1)$$

where $\vec{W}$ is a vector of conservative variables, $\vec{F}_c$ is a vector of convective fluxes, $\vec{F}_v$ is a vector of viscous fluxes, and $\vec{Q}$ is the source terms.

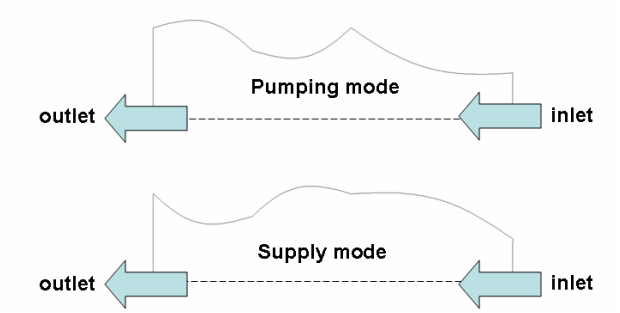

Figure 3: The micropump operating in pumping and supply modes. Arrows show the direction of fluid flow.

The working fluid of the micropump was assumed to be water with density of 998.2 kg/m^3 and viscosity of 959e-06 N.s/m^2. Since the thickness of the micropump was much less than other dimensions of the micropump, the flow can assumed to be constant in the thickness direction. The 2-D model of the half micropump, due to symmetry, was created in pre-processor software, GAMBIT. Triangular elements were used to represent this 2-D model in order to facilitate use of the dynamic mesh algorithm

A user-defined function was written in C complier to control the movement of the membrane. While the fluid-membrane interaction can affect the change in micropump volume, this effect is neglected in this study. The movement of the membrane was modeled using the first mode of vibrating string with two fixed edge. This movement is given by the following expression.

$$u(x,t)=A\sin\frac{\pi x}{L}\sin 2\pi ft \qquad (2)$$

where u is a membrane displacement (m), A is a maximum membrane displacement (m), x is a location along membrane length (m), L is membrane length (m), f is membrane frequency (Hz), and t is time (s).

The characteristic of micropump was evaluated by three input parameters; the maximum membrane displacement A, membrane frequency f, and pressure head ΔP. Pressure head $\Delta P = P_{out}-P_{in}$, where P_{in} and P_{out} are pressure levels at the inlet and outlet of the micropump. Transient simulations of the micropump were carried out at a maximum membrane displacement A from 0.25 to 1.50 mm, membrane frequency f from 1 to 500 Hz, and pressure

NSTI-Nanotech 2008, www.nsti.org, ISBN 978-1-4200-8505-1 Vol. 3

head ΔP from 0 to 5 kPa. In all cases, the simulations were performed until the flow rate at the outlet of the micropump reached a steady state solution. The solution for each time step was considered to be converged when residuals of mass and all velocity components were less than 10^{-6}.

4 MICROPUMP CHARACTERISTICS

4.1 Velocity Field and Flow Rate

The fluid velocity for the pumping and supply mode of the micropump operating with 1-mm membrane amplitude, 1-Hz membrane frequency and zero back pressure is shown in Figure 4. In contrast to the existing nozzle/diffuser micropump [4, 9], there is no back flow at the inlet during the pumping mode and there is no back flow at the outlet during the supply mode. The transient response of flow rate at the outlet of the micropump is shown in Figure 5. The maximum flow rate at the outlet of the micropump increased and reached a steady state after eight seconds (eight operating cycles). The maximum flow rate was about 36.93 μl/min. It is interesting to note that the flow rate of the micropump in this study was different from that of the nozzle/diffuser micropump, which had a retrograde flow rate throughout the operating cycle [4, 9].

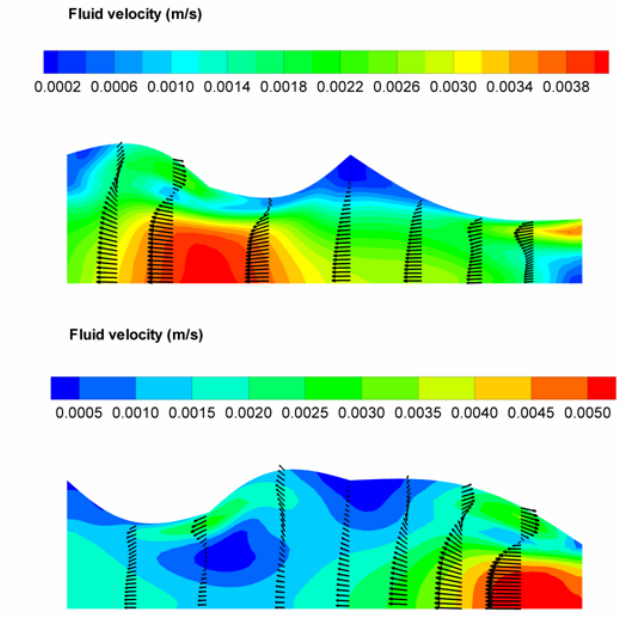

Figure 4: Velocity field within the micropump during the pumping (top) and supply (bottom) modes.

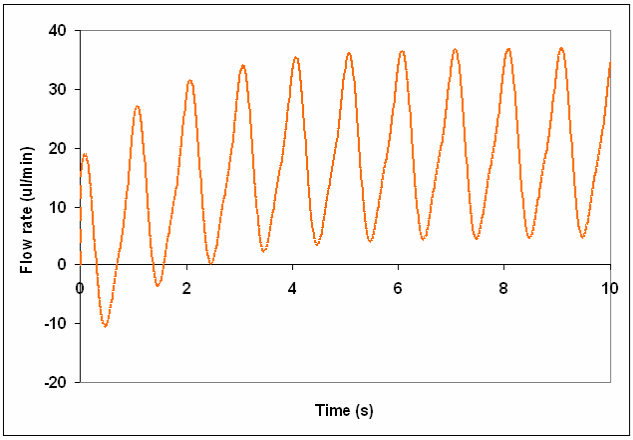

Figure 5: Flow rate at the outlet of the micropump with 1-mm membrane amplitude, 1-Hz membrane frequency and zero back pressure

4.2 Effects of Membrane Displacement

The transient responses of flow rate at the outlet of the micropump with zero pressure head and 1-Hz membrane frequency for four different maximum membrane displacements are plotted in Figure 6. The flow rate for all membrane displacements at the outlet of the micropump reached a steady state after eight seconds. As can be seen from this figure, this micropump should operate with maximum membrane displacement at least 0.50 mm to prevent a negative flow rate at the outlet. The maximum flow rates were 6.27, 15.56, 36.93, and 58.16 μl/min for 0.25-, 0.50-, 1.0-, and 1.5-mm maximum membrane displacement, respectively. The effect of the membrane amplitude on the proposed micropump was similar to that on nozzle/diffuser and peristaltic micropumps [10].

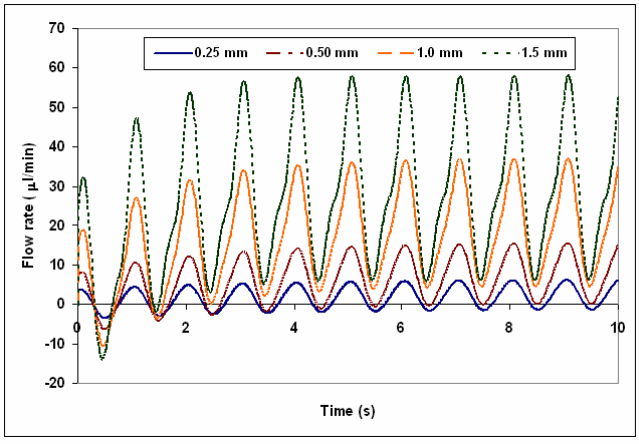

Figure 6: Flow rate at the outlet of the micropump with zero pressure head and 1-Hz membrane frequency for four different maximum membrane displacements.

4.3 Effects of Membrane Frequency

The flow rates at the outlet of the micropump with zero pressure head and 1.0-mm maximum membrane displacement for four different membrane frequencies are plotted in Figure 7. The flow rates for all membrane frequency had the same trend. The flow rate at the outlet of the micropump was a pulse flow and the negative flow rate only appeared in the first two operating cycle. The flow rate at the outlet of the micropump reached a steady state after eight operating cycles. There is no negative flow rate at a steady state. The maximum flow rate at the outlet increased when the membrane frequency increased. The maximum flow rates were 36.93, 435.33, 4731.06, and 24297.73 μl/min for 1-, 10-, 100-, and 500-Hz membrane frequency, respectively. The effect of the membrane frequency on the proposed micropump was similar to that on nozzle/diffuser and peristaltic micropumps [9-12].

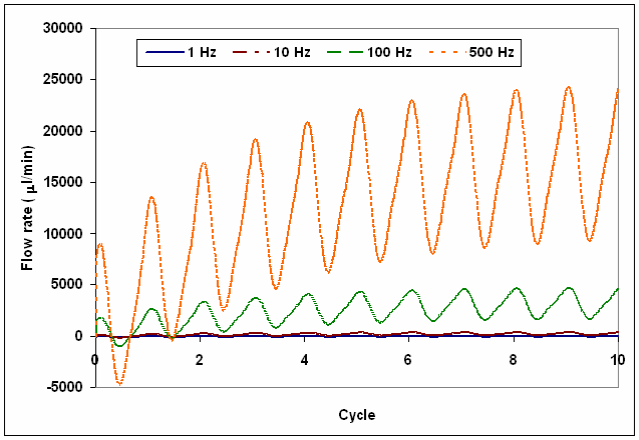

Figure 7: Flow rate at the outlet of the micropump with zero pressure head and 1.0-mm maximum membrane displacement for four different membrane frequencies.

5 CONCLUSION

Performance characteristics of a micropump with multiple vibrating membranes that are used to achieve a unidirectional flow were investigated in this study. This micropump uses the movement of multiple membranes and three nozzle/diffuser elements to improve fluid flow in one direction. The performance characteristics of the micropump were analyzed using a computational-based finite volume method. The fluid velocities and flow rates within the micropump were obtained through CFD simulations. The computational results showed that the maximum membrane displacement and membrane frequency were factors affecting the maximum flow rate of the novel micropump. The maximum flow rate increased when the maximum membrane displacement and frequency increased. Using the proposed design, retrograde flow was eliminated for most conditions that were considered. Based on these design simulations, a prototype of the micropump made of PDMS material will be studied in future.

ACKNOWLEDGEMENTS

The authors thank the US National Science Foundation for sponsoring the research reported in this study through a grant ECCS-0725496.

REFERENCES

[1] Cao, L., Mantell, S., and Polla, D., Sensors and Actuators A, 94, 117-125, 2001
[2] Jang, L., and Kan, W., Biomedical Microdevices, 9, 619-626, 2007
[3] Doll, A. F., Wischke, M., Geipel, A., Goldschmidtboeing, F., Ruthmann, O., Hopt, U. T., Schrag, H., and Woias, P., Sensors and Actuators A, 139, 203-209, 2007
[4] Singhal, V., and Garimella, S. V., IEEE Transactions on Advanced Packaging, 28, 216-230, 2005
[5] Zhang, T., and Wang, Q., Journal of Power Sources, 140, 72-80, 2005
[6] Beebe, D. J., Mensing, G. A., and Walker, G. M., Annual Reviews of Biomedical Engineering, 4, 261-286, 2002
[7] Woias, P., Sensors and Actuators B, 105, 28-38, 2005
[8] Blazek, J., "Computational Fluid Dynamics: Principles and Applications," Elsevier Ltd., 2005
[9] Yao, Q., Xu, D., Pan, L. S., Teo, A. L. M., Ho, W. M., Lee, V. S. P., and Shabbir, M., Engineering Application of Computational Fluid Mechanics, 1, 181-188, 2007
[10] Nguyen, N., and Huang, X., Sensors and Actuators A, 88, 104-111, 2001
[11] Goldschmidtboing, F., Doll, A., Heinrichs, M., Woias, P., Schrag, H. J., and Hopt, U. T., Journal of Micromechanics and Microengineering, 15, 673-683, 2005
[12] Huang, C., Huang, S., and Lee, G., Journal of Micromechanics and Microengineering, 16, 2265-2272, 2006